Electronic Supplementary Material (ESI) for Analyst.

Supporting Information

Discerning Toxic Nerve Gas Agents Via Distinguishable 'Turn-On' Fluorescence Response: Multi Stimuli Responsive Quinoline Derivatives in-Action

Sourav Mondal, [a] Bandarupalli Krishna, [a, b] Sounak Roy [a, c] and Nilanjan Dey[a]*

[a]Department of Chemistry, Birla Institute of Technology and Science Pilani, Hyderabad-500078, Telangana, India,

Email ID: nilanjandey.iisc@gmail.com, nilanjan@hyderabad.bits-pilani.ac.in

[b]Adama India Pvt. Ltd., Genome Valley, Hyderabad 500078, India

[c]Materials Center for Sustainable Energy & Environment, Birla Institute of Technology and Science Pilani Hyderabad Campus, Hyderabad, 500078, India

EXPERIMENTAL SECTION

Materials and Instrumentations All reagents and starting materials were obtained from the best-known commercial sources and were used without further purification. Solvents were distilled and dried prior to use. FTIR spectra were recorded on a Perkin-Elmer FT-IR Spectrum BX system and were reported in wave numbers (cm^{-1}). ^{1}H NMR and ^{31}P NMR spectra were recorded on a Bruker Advance DRX 400 spectrometer operating at 400 and 100 MHz for ^{1}H and ^{31}P NMR spectroscopy, respectively.

UV−Vis and Fluorescence Spectroscopy The UV−vis and fluorescence spectroscopy were recorded on a Shimadzu model 2100 spectrometer and Cary Eclipse spectrofluorimeter respectively. The slit widths were kept at 5 nm (excitation) and 5 nm (emission).

Dynamic Light Scattering Studies (DLS) DLS measurements were done using a Malvern Zetasizer Nano ZS particle sizer (Malvern Instruments Inc., MA) instrument. Samples were prepared and examined under dust-free conditions. Mean hydrodynamic diameters reported were obtained from Gaussian analysis of the intensity-weighted particle size distributions.

Detection limit determination. The method used for the calculation of the detection limit is known as the blank variation method. In this method, the calibration curve was prepared by fluorescence titration of $\mathbf{L_1}$ (10 μM) with DCNP and DClP in aqueous medium. The fluorescence signal of the compound without the added analytes was considered as blank reading. The standard deviation value was calculated from the blank readings and fluorescence titration data. Using this standard deviation value, we calculated limit of decision by this following equation.

$$L_C = t_C \times s \times (1 + 1/N)^{1/2} \quad \text{..... (1)}$$

where, N = the number of blank replicates taken; the value of tc for 10 blank readings is 1.833; and s = the standard deviation value. The detection limit (L_D) was calculated as the double of the decision limit obtained,

$$L_D = 2\,L_c \quad \text{..... (2)}$$

^{1}H NMR Titration Studies. ^{1}H NMR titration studies with probes $\mathbf{L_1}$ and $\mathbf{L_2}$ were performed (5 mM) in $DMSOd_6$ medium. To that DCNP and DClP were added (1:1) and the spectra were recorded using identical parameters. The chemical shifts have been represented as 'δ ppm'.

Scanning Electron Microscopy: Solution of $\mathbf{L_1}$ (concentration 10 μM) in water with and without DClP and DCNP were drop cast over double-sided tapes attached onto the brass stubs and air-dried for 48 h. The samples were then coated with gold vapor and analysed on a Quanta 200 SEM operated at 15 kV.

Additional Spectroscopic Data

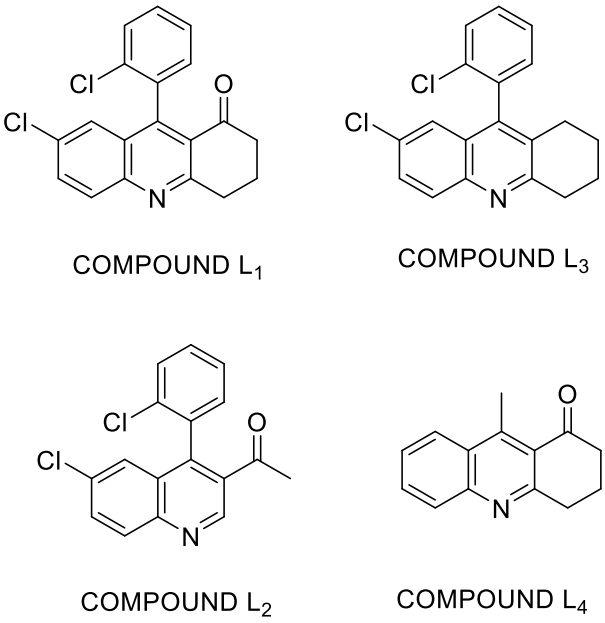

Fig. S1 (a) Structures of compounds (**L_1** to **L_4**) involved in the present study. (b) Chemical structures of analytes screened in the present study.

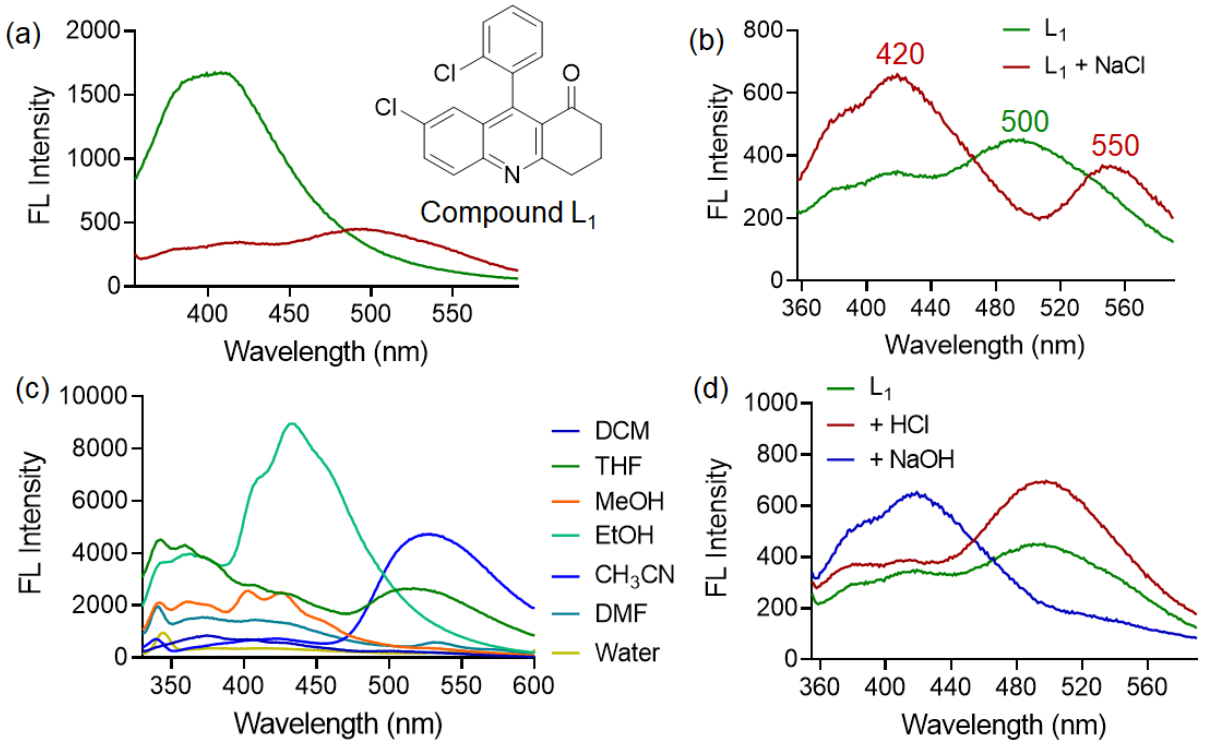

Fig. S2 (a) Fluorescence spectra of **L_1** (10 μM, λ_{ex} = 340 nm) in water and water-glycerol mixture (20:80) medium. (b) Fluorescence spectra of **L_1** (10 μM, λ_{ex} = 340 nm) in water medium with and without NaCl (7 M). (c) Fluorescence spectra of **L_1** (10 μM, λ_{ex} = 340 nm) in different organic medium. (d) Fluorescence spectra of **L_1** (10 μM, λ_{ex} = 340 nm) in presence of acid and alkali in the aqueous medium.

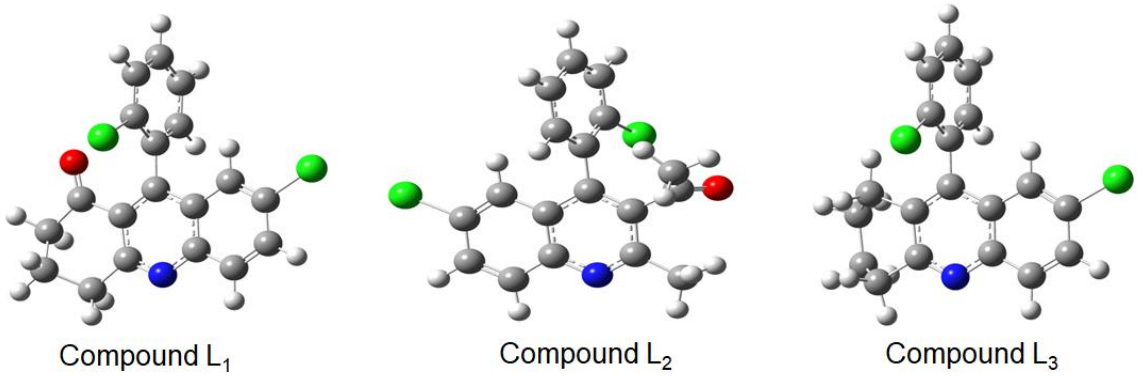

Fig. S3 Energy optimized structures of compounds (**L_1** to **L_3**) using B3LYP/6-31G* level of theory.

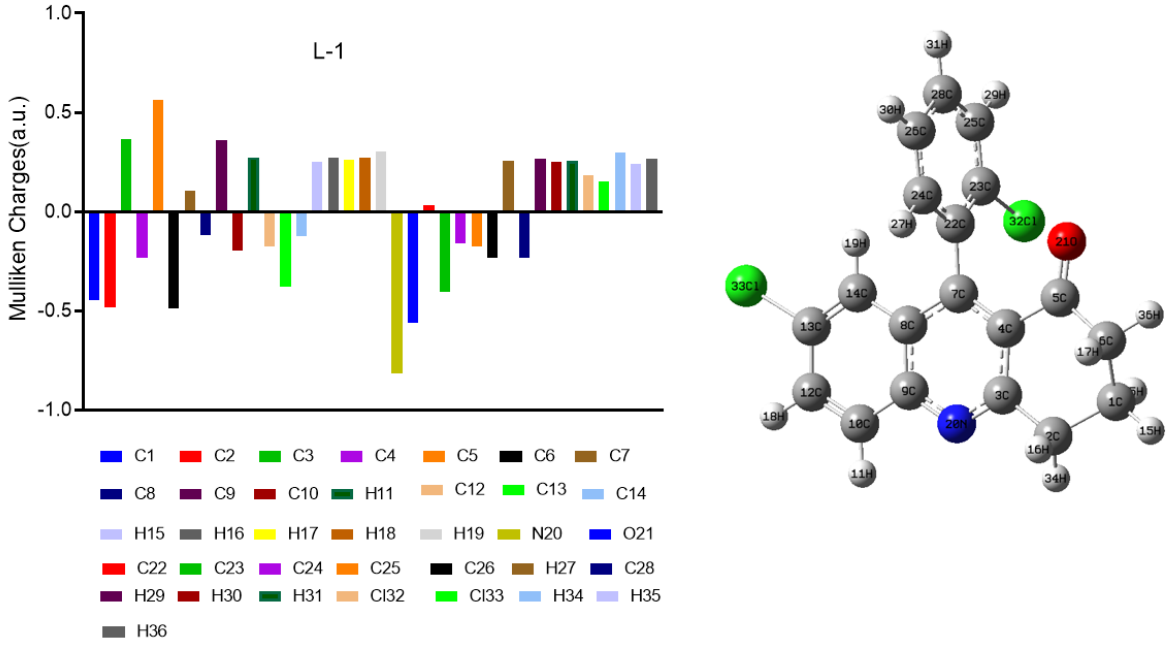

L-2

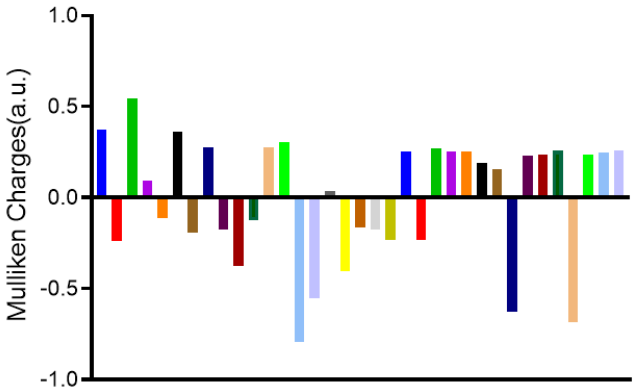

C1 C2 C3 C4 C5 C6 C7
H8 C9 C10 C11 H12 H13 N14
O15 C16 C17 C18 C19 C20 H21
C22 H23 H24 H25 Cl26 Cl27 C28
H29 H30 H31 C32 H33 H34 H35

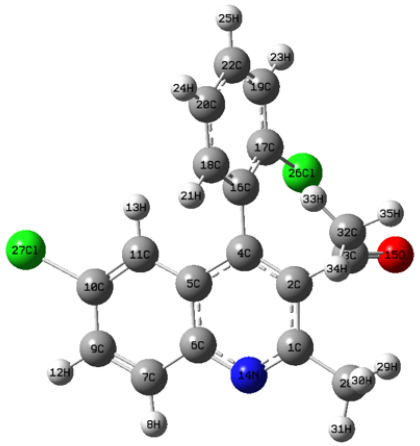

L-3

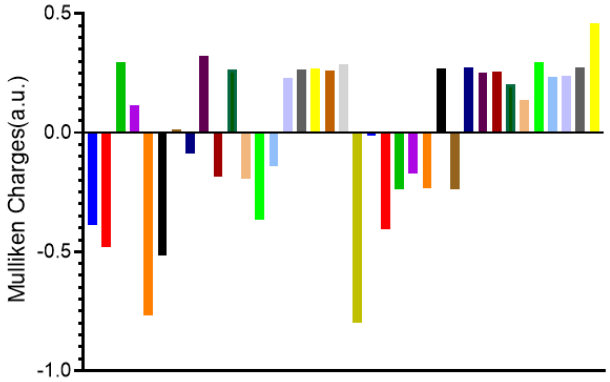

C1 C2 C3 C4 C5 C6 C7
C8 C9 C10 H11 C12 C13 C14
H15 H16 H17 H18 H19 N20 C21
C22 C23 C24 C25 H26 C27 H28
H29 H30 Cl31 Cl32 H33 H34 H35
H36 H37

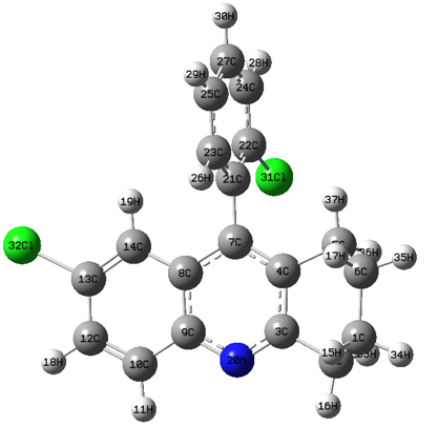

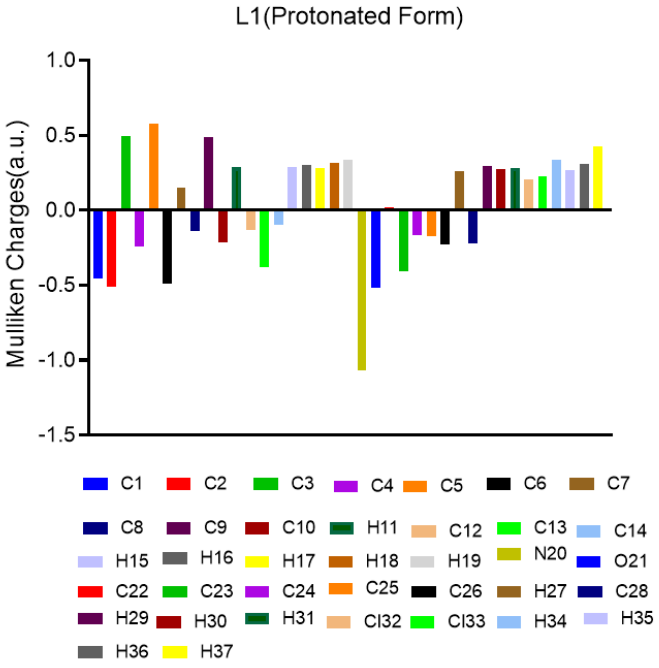
L1(Protonated Form)
Mulliken Charges(a.u.)
1.0
0.5
0.0
-0.5
-1.0
-1.5
C1 C2 C3 C4 C5 C6 C7
C8 C9 C10 H11 C12 C13 C14
H15 H16 H17 H18 H19 N20 O21
C22 C23 C24 C25 C26 H27 C28
H29 H30 H31 Cl32 Cl33 H34 H35
H36 H37

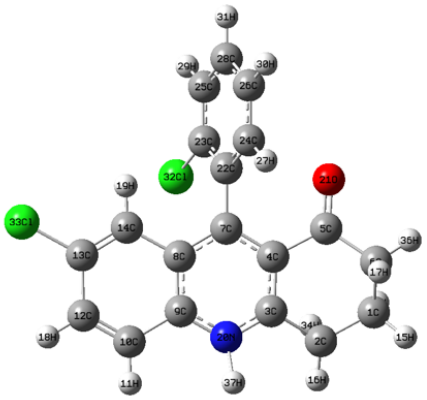

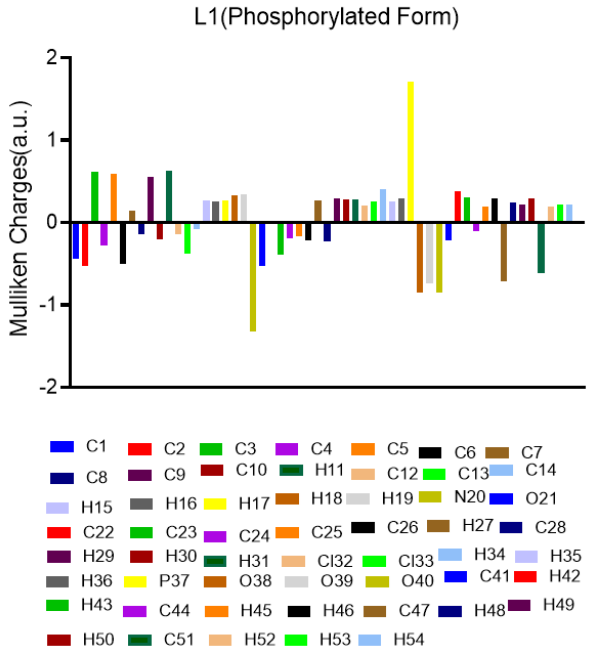
L1(Phosphorylated Form)
Mulliken Charges(a.u.)
2
1
0
-1
-2
C1 C2 C3 C4 C5 C6 C7
C8 C9 C10 H11 C12 C13 C14
H15 H16 H17 H18 H19 N20 O21
C22 C23 C24 C25 C26 H27 C28
H29 H30 H31 Cl32 Cl33 H34 H35
H36 P37 O38 O39 O40 C41 H42
H43 C44 H45 H46 C47 H48 H49
H50 C51 H52 H53 H54

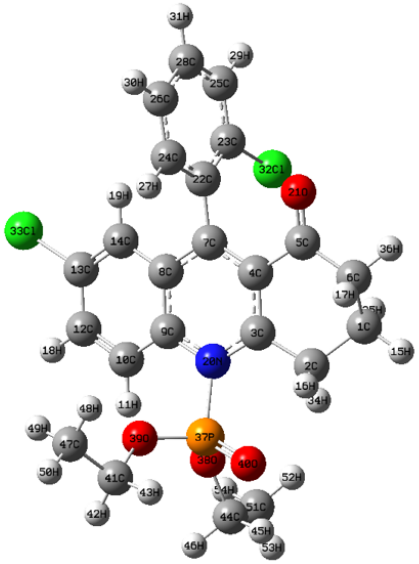

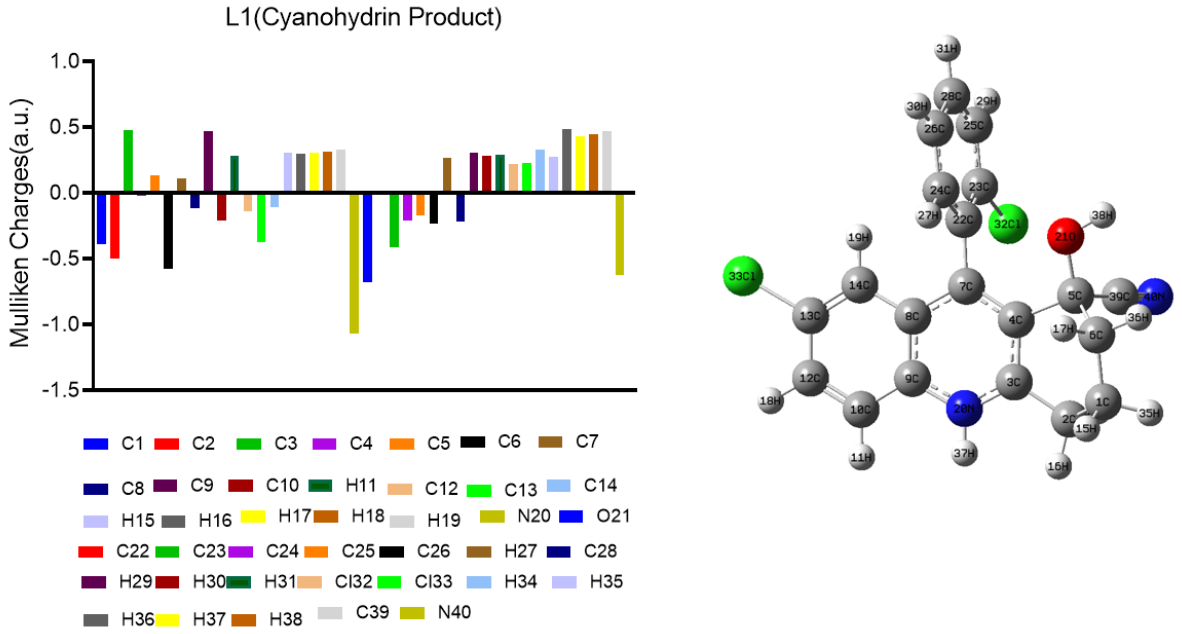

Fig. S4 Optimized structures, Mulliken charges distribution plots of **L1, L2, L3** and protonated phosphorylated, cyanohydrin form of $\mathbf{L_1}$.

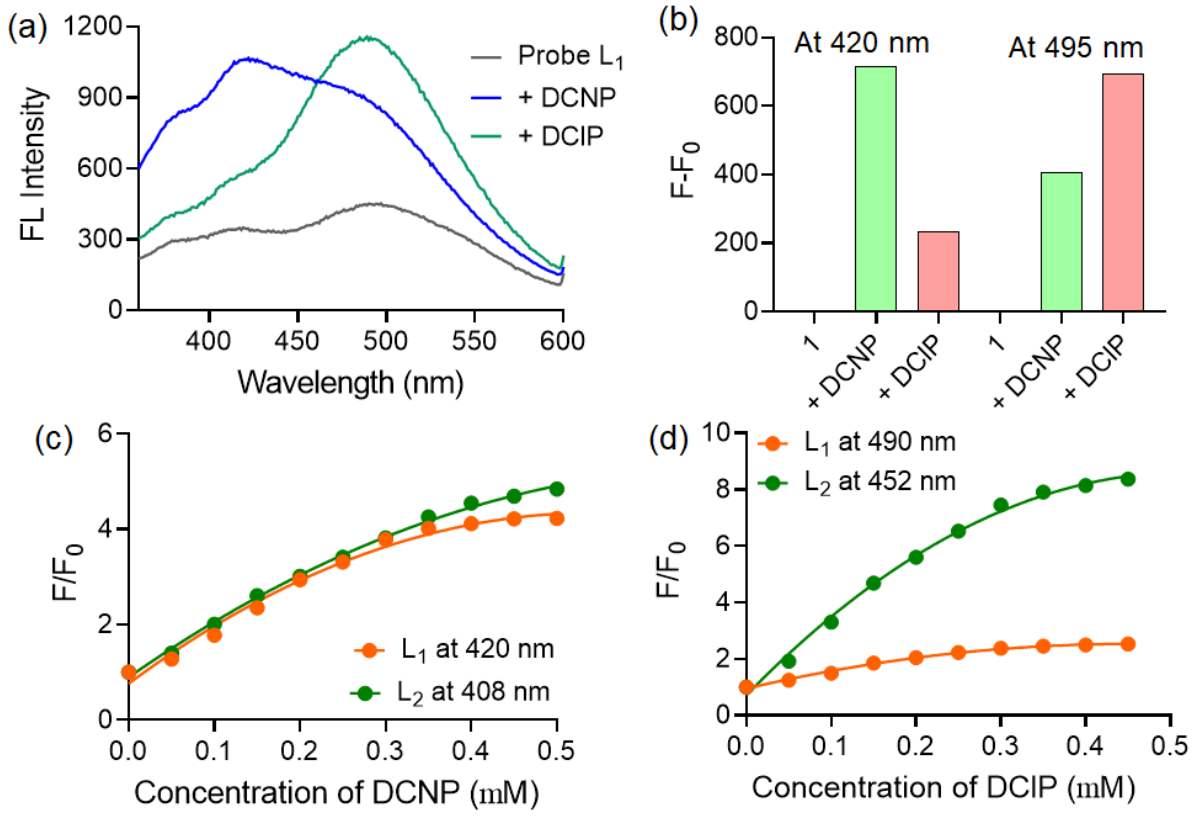

Fig. S5 (a) Fluorescence spectra of $\mathbf{L_1}$ (10 μM, λ_{ex} = 340 nm) with DCIP and DCNP in aqueous medium. (b) Change in fluorescence intensity of $\mathbf{L_1}$ (10 μM, λ_{ex} = 340 nm) with DCIP and DCNP (0.5 mM) at 495 and 420 nm in aqueous medium. (d) Change in fluorescence intensity of $\mathbf{L_1}$ and $\mathbf{L_2}$ (10 μM, λ_{ex} = 340 nm) upon addition of DCNP (0 – 0.5 mM) in the aqueous medium. (d) Change in fluorescence intensity of $\mathbf{L_1}$ and $\mathbf{L_2}$ (10 μM, λ_{ex} = 340 nm) upon addition of DCIP (0 – 0.5 mM) in the aqueous medium.

Compound	Quantum Yield (Φ)	With DCLP	With DCNP
L1	0.0047	0.0093	0.0184
L2	0.0057	0.0079	0.011
L3	0.0054	-	-

Table S1: Quantum Yield of compounds L1, L2 and L3 with DCLP and DCNP

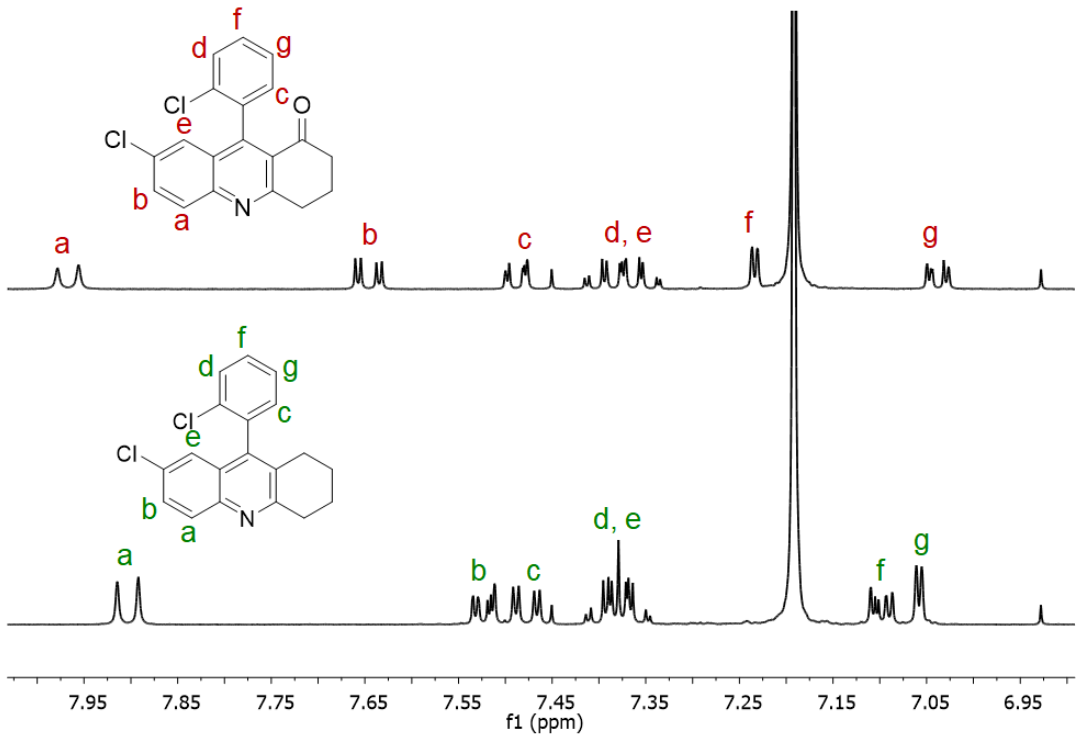

Fig. S6 Partial ^{1}H-NMR spectra of $\mathbf{L_1}$ and $\mathbf{L_2}$ (5 mM) in DMSO-d_6 medium.

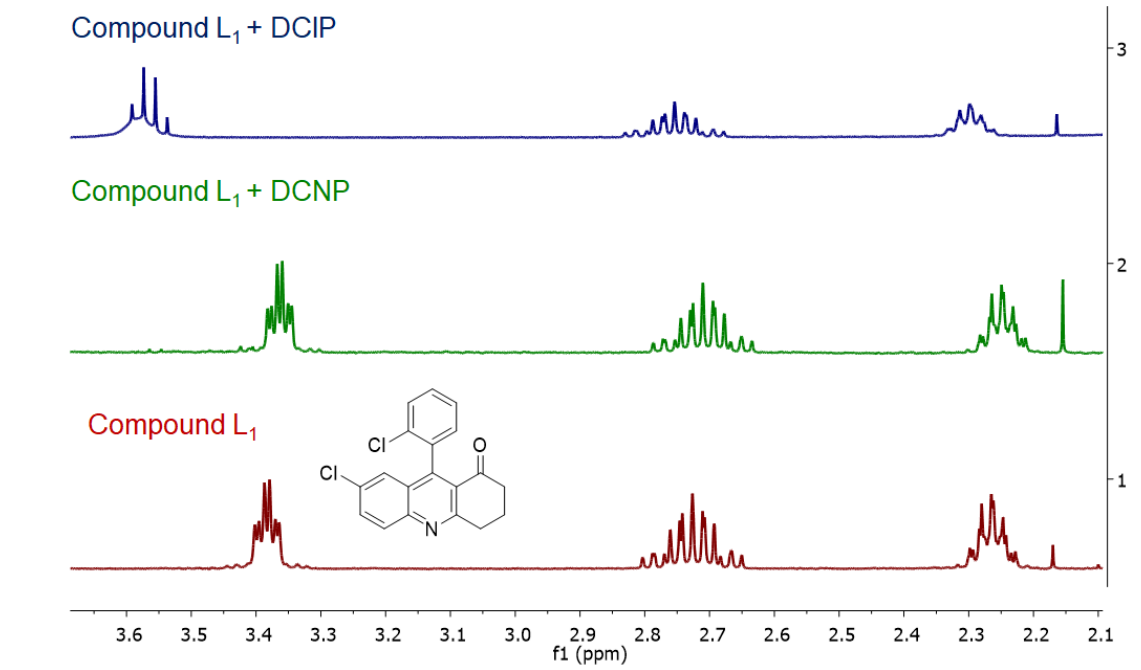

Fig. S7 Partial ^{1}H-NMR spectra of **L_1** (5 mM) with DCIP and DCNP in DMSO-d_6 medium.

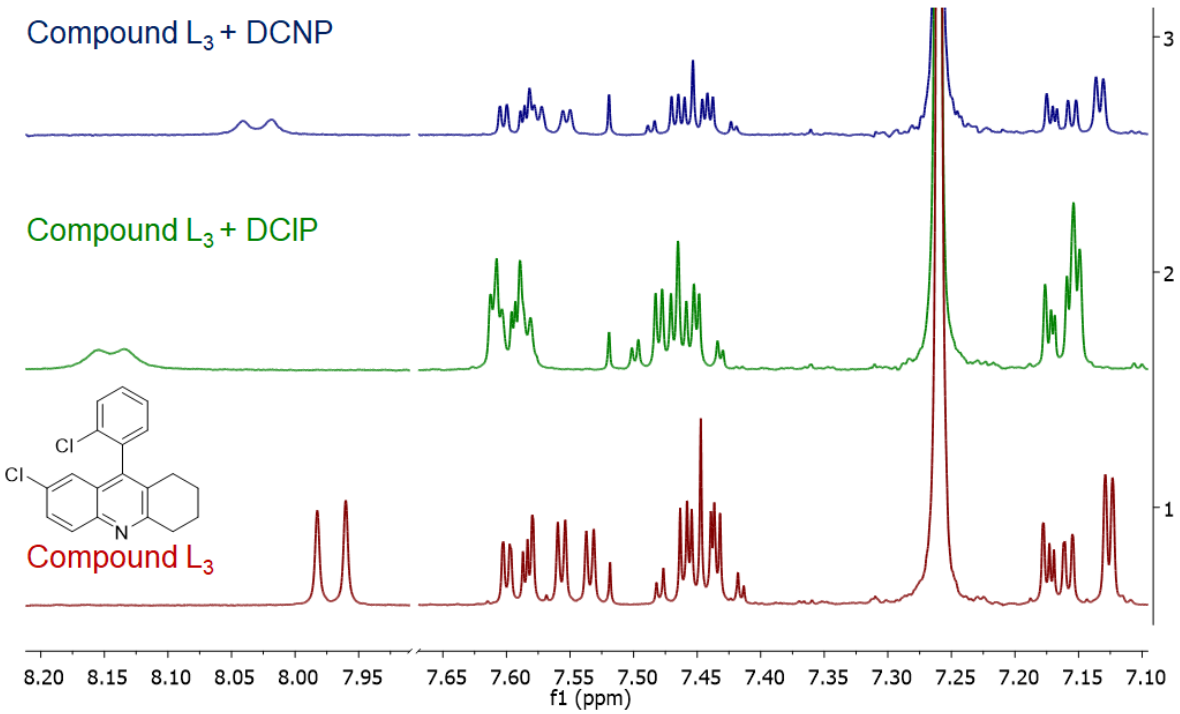

Fig. S8 Partial ^{1}H-NMR spectra of **L_3** (5 mM) with DCIP and DCNP in DMSO-d_6 medium.

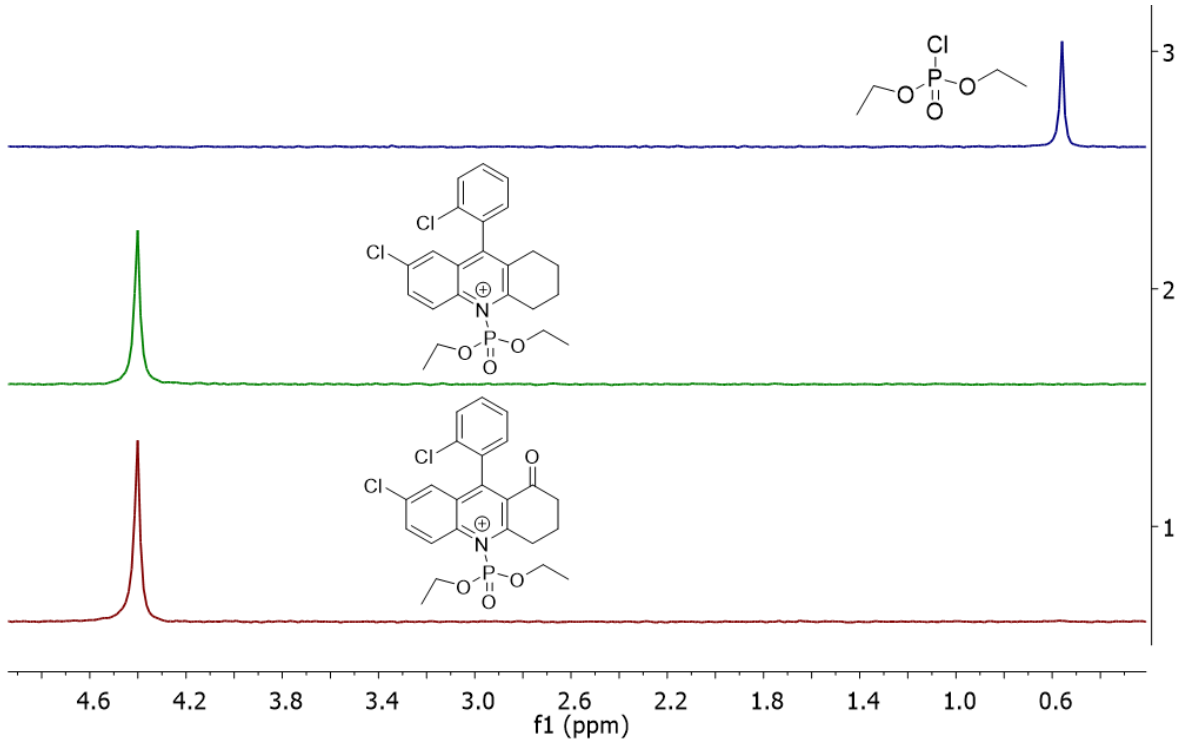

Fig. S9 ^{31}P-NMR spectra of **L_1** and **L_3** (5 mM) with DCIP in DMSO-d_6 medium.

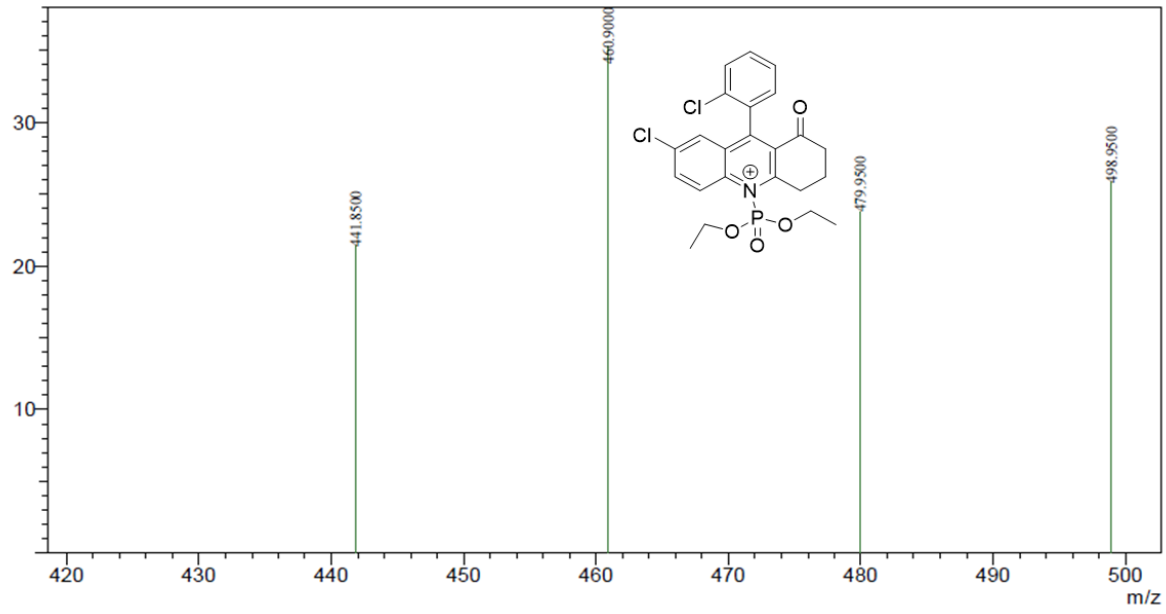

Fig. S10 ESI-MS spectra of **L_1** with DCIP in the aqueous medium.

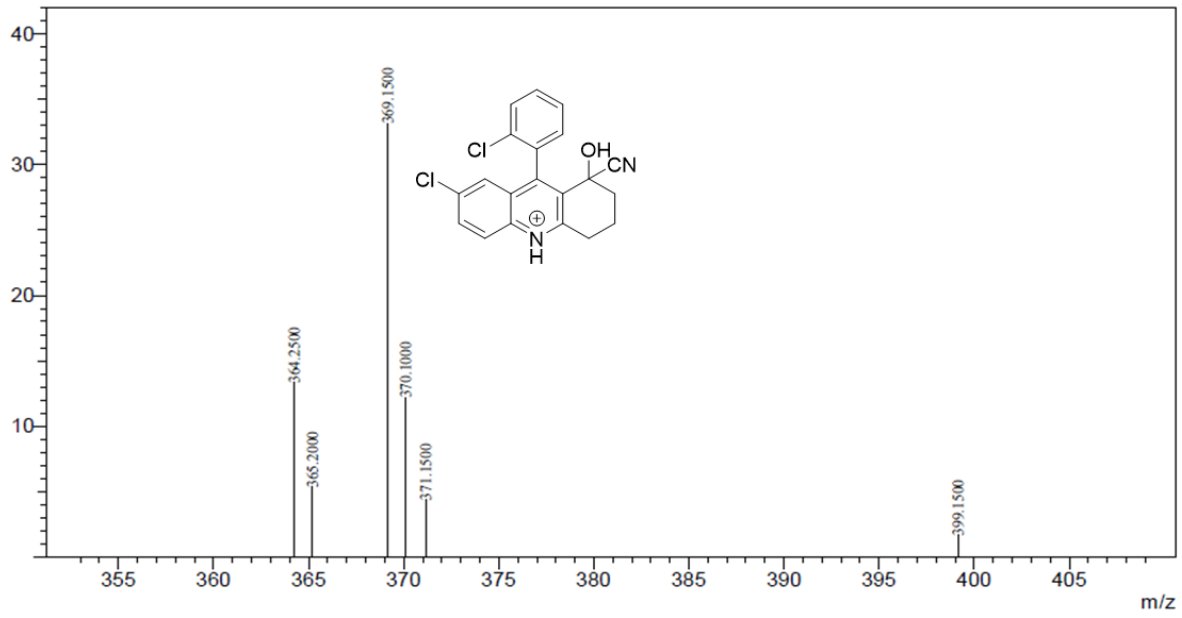

Fig. S11 ESI-MS spectra of $\mathbf{L_1}$ with DCNP in the aqueous medium.

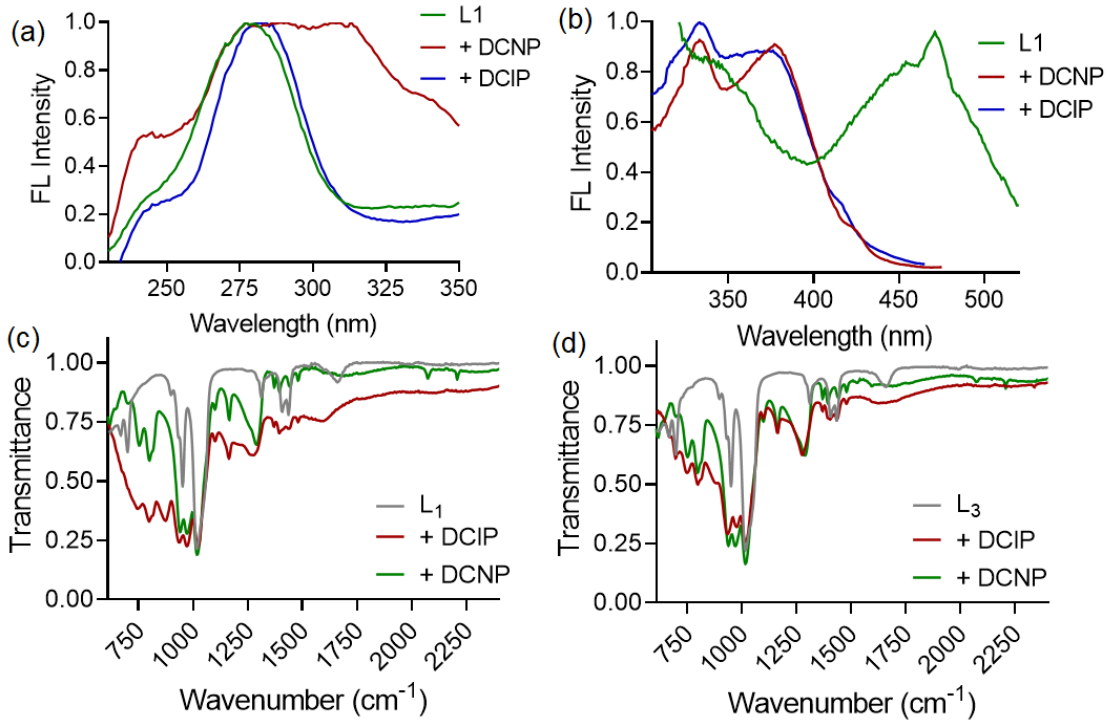

Fig. S12 Fluorescence excitation spectra of $\mathbf{L_1}$ (10 μM) with DCIP and DCNP (a) at 420 nm and (b) 495 nm in aqueous medium. FT-IR spectra of (c) $\mathbf{L_1}$ (d) $\mathbf{L_2}$ (0.5 mM) with DCIP and DCNP in aqueous medium.

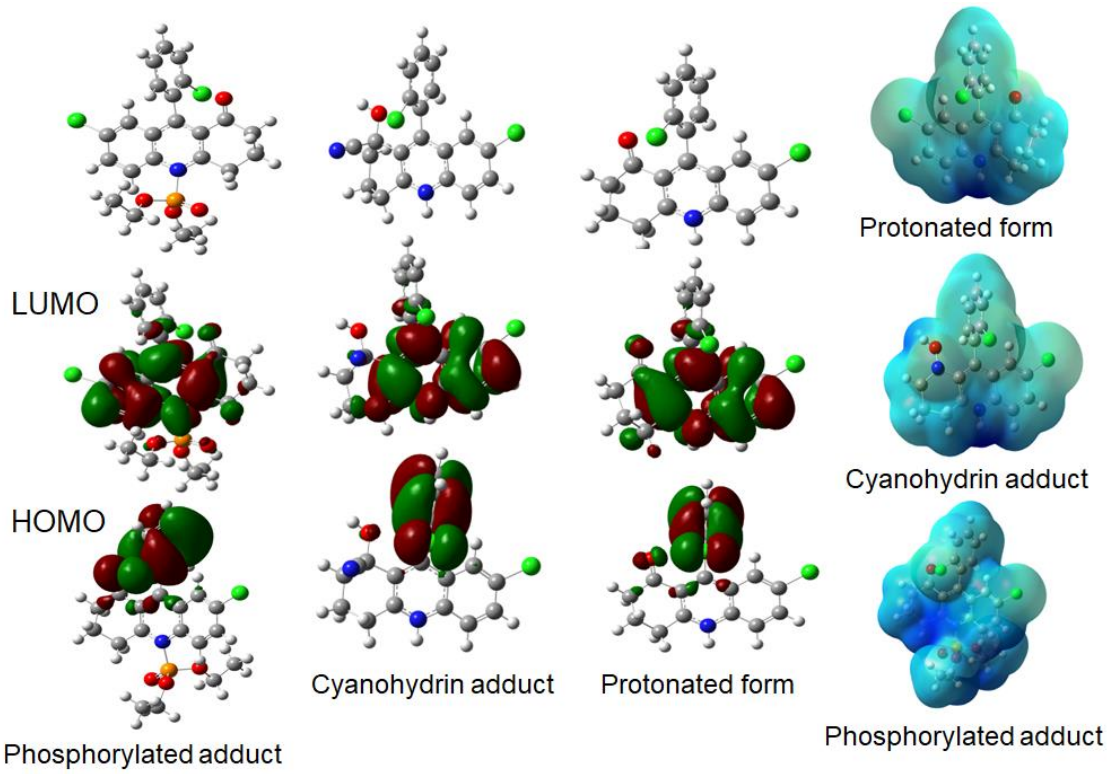

Fig. S13 Optimized structures, electrostatic potential maps, and frontier orbital analysis of phosphorylated adduct, cyanohydrin derivative and protonated form of $\mathbf{L_1}$.